

# Synthesis of single silica nanotubes in the presence of citric acid

Lianzhou Wang,\* Shinji Tomura, Fumihiko Ohashi, Masaki Maeda, Masaya Suzuki and Keiichi Inukai

Ceramic Technology Dept., National Industrial Research Institute of Nagoya, 1-1 Hirate, Kita-ku, Nagoya 462-8510, Japan

Received 20th December 2000, Accepted 13th February 2001  
First published as an Advance Article on the web 16th March 2001

Citric acid has been employed as a structural modifier for the first time to synthesize single silica nanotubes *via* a sol-gel process at room temperature. XRD results reveal the amorphous nature of the silica framework. SEM and TEM images show that the nanotubes were 0.5–20  $\mu\text{m}$  in length, and 50–500 nm in width. TG-DTA and FTIR results indicate that the possible interaction between citric acid molecules and inorganic species should be very weak. The structural direction of ammonium citrate crystals under appropriate synthetic conditions was argued to explain the formation of particular morphologies.

## Introduction

Recently, much attention has been focused on novel porous materials<sup>1–3</sup> because of their potential wide-ranging applications in catalysis, adsorption, nanotechnology, *etc.* Compared with the synthesis of porous materials with integrated structures, the preparation of single or free nanotubes is another major challenge. With the exception of well-known carbon nanotubes,<sup>3</sup> which are usually synthesized by high-temperature techniques, most inorganic oxide single nanotubes have been prepared by using template and sol-gel processing. There are two main pathways for the synthesis of oxide nanotubes. One straightforward method was conducted by employing some porous or fibrous materials as templates, *e.g.* carbon nanotubes,<sup>4–6</sup> nanoporous membranes,<sup>7,8</sup> *etc.*, to guide the formation of single oxide nanotubes. Tubules of  $\text{SiO}_2$ ,  $\text{Al}_2\text{O}_3$ ,  $\text{ZrO}_2$ ,  $\text{MoO}_3$ ,  $\text{TiO}_2$  and  $\text{V}_2\text{O}_5$  have been obtained *via* this “direct” template method. The other method involves the use of organic molecules, where the interaction and/or self-assembly between inorganic precursors and organic templates may offer unique alternatives in the development of inorganic nanotube materials. So far, some organic templates, such as long chain surfactants<sup>9,10</sup> and organogelators,<sup>11,12</sup> *etc.*, have been utilized to prepare oxide nanotubes.

Recently, simple organic hydroxycarboxylic acids, in particular *dl*-tartaric acid,<sup>13</sup> have been used to prepare silica nanotubes in an ethanol/water/ $\text{NH}_4\text{OH}$ /tetraethyl orthosilicate (TEOS) reaction system under static conditions. Mann *et al.*<sup>14</sup> developed the method and considered that needle-like crystals of organic salts had contributed to the formation of nanotubes, even though there were large differences in particle sizes between ammonia tartrate crystals and nanotubes. In this work, we demonstrate a new procedure to synthesize silica nanotubes using citric acid (CA) as a structural modifier for the first time. It has been found that the morphologies of products were sensitive to the synthetic conditions. Rapid addition of ammonia and CA under static conditions gives only uniform micrometer-sized rods with well-defined morphologies. However, the slow addition of ammonia/CA under stirring was effective for the formation of single nanotubes. Both the use of citric acid and external synthetic conditions are responsible for the formation of particular forms of silica.

## Experimental

### Preparation

The silica nanotubes were synthesized at room temperature. Ethanol, water and TEOS, ammonia and citric acid monohydrate were used as chemical sources. In a typical synthetic procedure, 6.0 ml of TEOS was added to the mixed solution of 0.7 ml of  $\text{H}_2\text{O}$  and 30 ml of EtOH; and then 12 ml of  $\text{NH}_4\text{OH}$  (28% aqueous solution) containing 0.18 g of CA monohydrate were added dropwise into the homogenous solution in 2 h under magnetic stirring with a speed of *ca.* 300 rpm. After the mixed gel was loaded quietly for another 2 h, the precipitate was centrifugal washed with distilled water and dried in an oven at 75 °C; finally the product was calcined at 500 °C for 2 h to obtain silica nanotube materials. For comparison, additional silica materials in the absence or with different amounts of CA were also synthesized according to the similar procedure.

### Characterization

Transmission electron microscopy images were observed with a JEOL-200 CX electron microscope. The scanning electron micrographs were obtained from a Hitachi S-3500N SEM instrument. X-Ray powder diffraction measurements were carried out on a Rigaku RINT 2000 diffractometer.  $\text{N}_2$  adsorption-desorption isotherms, BET surface areas and BJH pore size distributions were determined using a Sorptomatic 1900 analyzer. Thermogravimetric analysis (TG-DTA) was performed on a Seiko RTG-320U instrument with a heating rate of 5 °C  $\text{min}^{-1}$ . FTIR spectra were collected on Perkin Elmer FT-IR Spectrum 2000 equipment.

## Results and discussion

Fig. 1a gives the TEM image of nanotubes. It is shown that numbers of long single nanotubes together with some nanoparticles coexisted in the materials. The outer diameter of nanotubes varied from 50 to 500 nm with the majority around 100–150 nm. The length of tubes ranged from hundreds of nanometers up to tens of micrometers. From the high-magnification image of a typical nanotube (Fig. 1b), it can be seen that the center of the material is light and both edges are

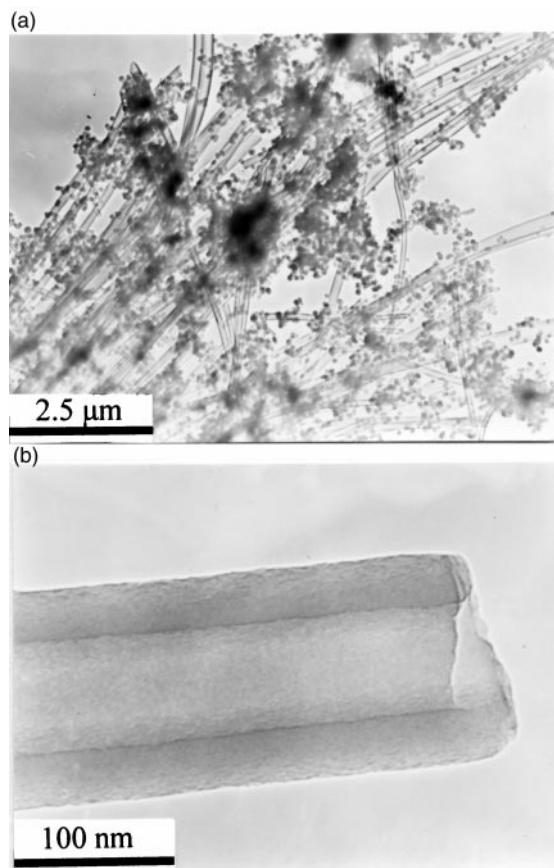


**Fig. 1** Low-magnification (a) and high-magnification (b) TEM images of single silica nanotubes.

dark, showing the well-defined structure of the nanotube. The inner and outer diameters of the tubes are about 65 nm and 130 nm respectively; and the thickness of the silica wall is *ca.* 30 nm. The head part of the tube indicates that the channel is open. The yields of nanotubes can be observed from the low-magnified SEM image (Fig. 2a). In contrast, silica materials synthesized using a similar procedure but in the absence of CA gave only sub-micrometer sized particles, indicating the particular effect of CA in the formation of silica nanotubes. Moreover, stirring is another key factor to influence the morphologies of materials. Fig. 2b gives a SEM picture of a sample synthesized by rapid addition of ammonia without stirring. It can be seen that the materials have the morphologies of uniform bone-like rods rather than nanotubes or nanoparticles. Meanwhile, the samples obtained by rapid addition of ammonia followed by stirring for 2 h give only nanoparticles. Therefore, the synthetic conditions also influence the particular morphologies of materials.

Powder XRD diffraction patterns of uncalcined (a) and calcined nanotubes (b) in Fig. 3 show that only one broad peak appears at about 23–24°, indicating that the silica framework is amorphous. The N<sub>2</sub> isotherm of a calcined sample (Fig. 4) shows that an extremely steep increase of the N<sub>2</sub> adsorbed volume in the adsorption isotherm occurs at the high N<sub>2</sub> relative pressure between 0.85 and 1, the reason might be due to the capillary condensation of liquid N<sub>2</sub> in the nanosized channels together with some inter-particle contribution. The isotherm is basically of type IV with a H1 type-like hysteresis loop, indicating the existence of tubular mesoporosity in the materials. The BET surface area of the material based on the N<sub>2</sub> isotherms is only 15.5 m<sup>2</sup> g<sup>-1</sup>, however the pore volume of the material is comparable high, about 0.21 cm<sup>3</sup> g<sup>-1</sup>, implying a contribution from the large inner space of the nanotubes. The BJH pore size distribution of the sample reveals a bimodal pore size distribution in the material: one with an average pore

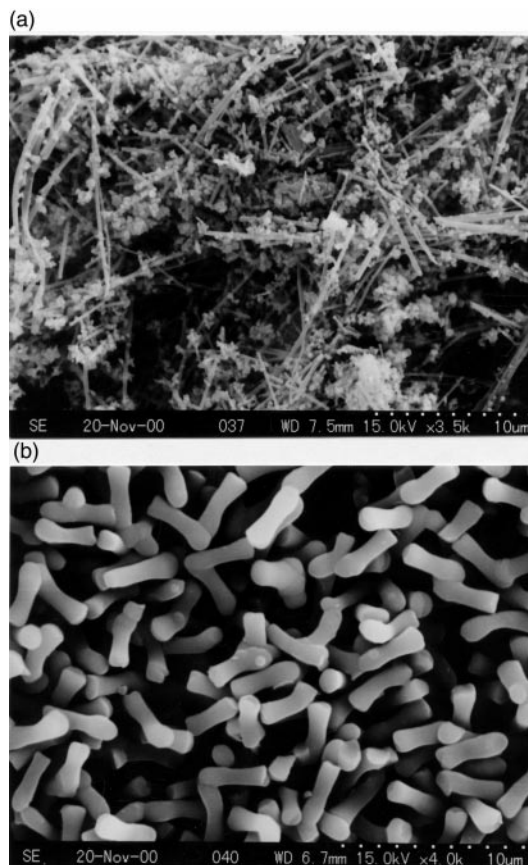


**Fig. 2** SEM images of silica nanotubes (a) and micrometer-sized bonelike rods (b).

diameter of about 5.6 nm, which might be attributed to the mesopores within the amorphous walls of nanotubes and nanoparticles; the other centered with a pore size at *ca.* 58 nm, confirming the cavities of nanotubes.

In the experiments, FTIR and TG-DTA were employed to investigate the possible role of CA in the formation of nanotubes. Comparing with the DTA result of a sample obtained in the absence of CA (Fig. 5a), a subtle exothermic peak (arrow) can be discerned around 300 °C in water washed nanotubes (Fig. 5b); meanwhile, the same sample dried without any water washing process provides a stronger signal for the decomposition of organic CA molecules than that of the washed sample (arrow in Fig. 5c), indicating that the unwashed sample may contain more CA molecules. Perhaps due to the small amounts of CA in the materials, no obvious differences among the samples can be identified in the TG curves. The FTIR spectrum (Fig. 6a) of a sample prepared in the absence of CA has the peaks characteristic of an amorphous silica material. An additional vibration band at *ca.* 1402 cm<sup>-1</sup> can

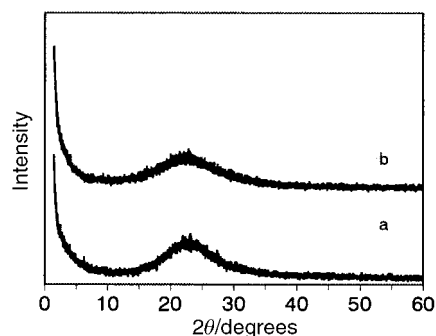


**Fig. 3** Powder XRD patterns of uncalcined (a) and calcined (500 °C) silica nanotubes.

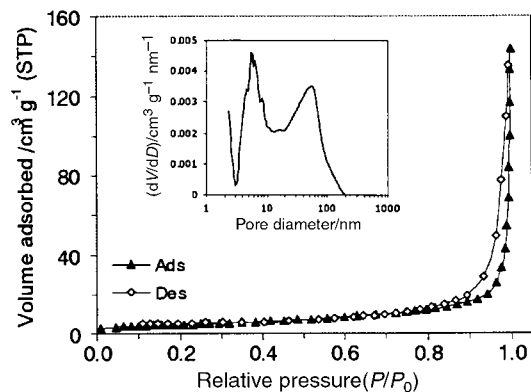


Fig. 4 Nitrogen adsorption-desorption isotherm of silica nanotube material and its BJH differential pore size distribution (inserted).

be observed in the curves of washed and unwashed nanotubes (Fig. 6b and c), which should be due to the symmetric C–O stretching mode of the carboxylate group.<sup>15</sup> Both TG-DTA and FTIR results imply that some of the organic CA molecules in CA-containing samples can be removed by a water washing process. Therefore, the possible interaction between organic species CA and silica precursors in the reaction system should be very weak.

In order to investigate the possible formation mechanism of particular silica morphologies, it should be helpful to examine the crystal structure of ammonium citrate crystals. The precipitate of ammonium citrate crystals can be rapidly obtained according to a similar process as for nanotube preparation but in the absence of TEOS. The SEM image of ammonium citrate (Fig. 7a) shows that most of the crystals have pillar-like morphologies. Since the melting point of

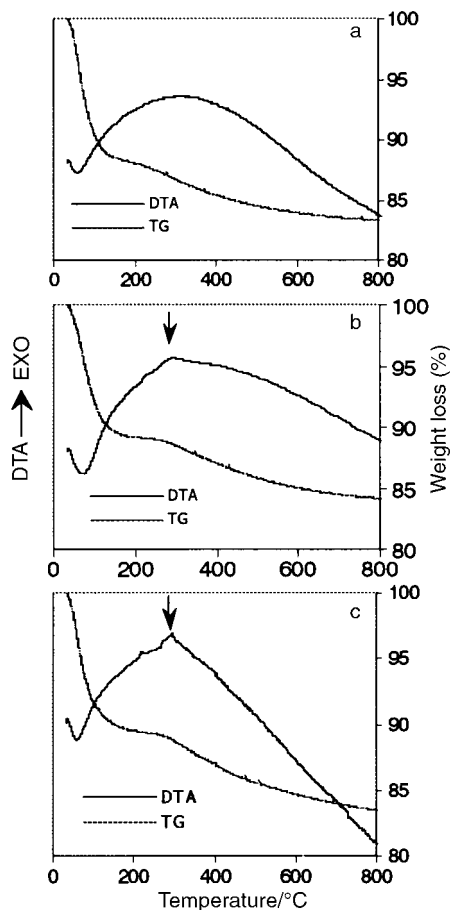


Fig. 5 TG-DTA curves of uncalcined silica materials. a: sample synthesized in the absence of CA; b: water washed nanotubes; c: unwashed nanotubes.

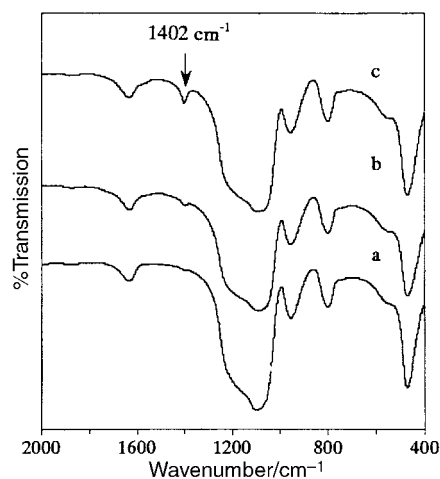


Fig. 6 FTIR spectra of uncalcined silica materials. a: sample synthesized in the absence of CA; b: washed nanotubes; c: unwashed nanotubes.

ammonium citrate is rather low, it is very easy to destroy the surface morphologies of materials during SEM observation. Though the surfaces of some particles have been melted in the image of Fig. 7b, there is an intact crystal of ammonium citrate (arrow) with perfect crystal faces and a small cavity in the pillar-like particle. It has been considered that the needle-shaped hollow fibers of ammonium tartrate crystals could be the template in the formation of silica nanotubes.<sup>14</sup> In the present work, we also think that the particular morphology of ammonium citrate may act as a structural modifier in the preparation of particular morphologies. However, the great

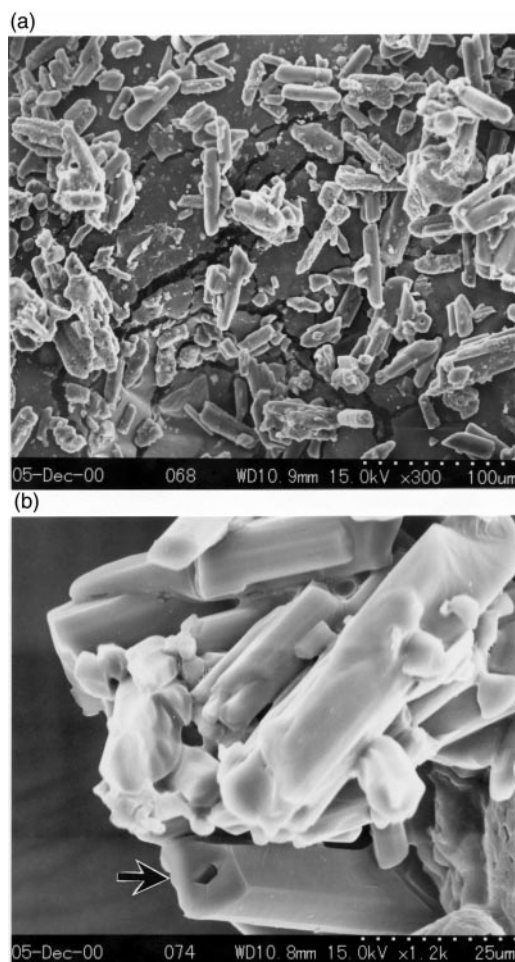


Fig. 7 SEM images of ammonium citrate crystals (a) and one typical intact crystal (b) (arrow) synthesized in the absence of TEOS.

differences between nanotubes and bonelike rods, both in morphologies and particle sizes (Fig. 2), remind us that some other factors should also be considered to explain the phenomena.

It was believed that quiescent conditions could be a key role in the formation of some particular morphology.<sup>16</sup> In this work, the formation of well-defined micrometer-sized rods seems to be another example directed by the organic species. Since hydroxycarboxylic groups could affect the hydrolysis and condensation processes of TEOS,<sup>17,18</sup> there is the chance for the active groups of ammonium citrate crystals to interact with silanol groups of silica species *via* weak interactions during the sol-gel processing; meanwhile, the structures of ammonium citrate crystals formed in quiescent conditions provide oriented attachable sites for silica species to anchor. Therefore, the natural outgrowth of silica nucleation guided by ammonium citrate crystal structures might finally lead to the particular rods. As to the formation of nanotubes, other factors should be regarded together with the contribution of ammonium citrate. Though the ammonium citrate crystals have the tendency of oriented growth in reaction systems during slow addition of ammonia/CA, its process will inevitably be disturbed by the external force of stirring. Therefore, the guided nucleation and outgrowth process of silica will also be agitated. Two factors, the inclination of oriented growth and the tendency of disorder, coexist and duel in the reaction system. The results of synergetic effects may finally lead to the compromised products of mixed nanotubes/nanoparticles other than uniform micrometer-sized rods.

## Conclusions

Citric acid has been employed as a structural modifier to guide the formation of single silica nanotubes and micrometer-sized rods. Careful control of synthetic conditions is essential for the formation of particular morphologies. The processing may be applied to other materials to allow their shape control, though the intrinsic mechanism for the formation of specific shapes needs further study.

## Acknowledgements

One of the authors (L. Wang) deeply appreciates the Japan International Science and Technology Center for the award of a STA fellowship.

## References

- 1 C. T. Kresge, M. E. Leonowicz, W. J. Roth, J. C. Vartuli and J. S. Beck, *Nature*, 1992, **359**, 710.
- 2 Q. Huo, D. Margolese, U. Ciesla, P. Feng, T. Gier, P. Sieger, R. Leao, P. M. Petroff, F. Schuth and G. D. Stucky, *Nature*, 1994, **368**, 317.
- 3 A. Iijima, *Nature*, 1992, **254**, 56.
- 4 P. M. Ajayan, O. Stephan, Ph. Redlich and C. Colliex, *Nature*, 1995, **375**, 564.
- 5 C. N. R. Rao, B. C. Satishkumar and A. Govindaraj, *Chem. Commun.*, 1997, 1581.
- 6 B. C. Satishkumar, A. Govindaraj, E. M. Vogl, L. Basumallick and C. N. R. Rao, *J. Mater. Res.*, 1997, **12**, 604.
- 7 B. B. Lakshmi, P. K. Dorhout and C. R. Martin, *Chem. Mater.*, 1997, **9**, 857.
- 8 (a) M. Zhang, Y. Bando, K. Wada and K. Kurashima, *J. Mater. Sci. Lett.*, 1999, **18**, 1911; (b) M. Zhang, Y. Bando and K. Wada, *J. Mater. Res.*, 2000, **15**, 387.
- 9 M. Adachi, T. Harada and M. Harada, *Langmuir*, 1999, **15**, 7097.
- 10 H. Muhr, F. Krumeich, U. P. Schonholzer, F. Bieri, M. Niederberger, L. J. Gauchler and R. Nesper, *Adv. Mater.*, 2000, **12**, 231.
- 11 Y. Ono, K. Nakashima, M. Sano, Y. Kanekiyo, K. Inoue, J. Hojo and S. Shinkai, *Chem. Commun.*, 1998, 1477.
- 12 S. Kobayashi, K. Janabusa, N. Hamasaki, M. Kimura and H. Shirai, *Chem. Mater.*, 2000, **12**, 1523.
- 13 H. Nakamura and Y. Matsui, *J. Am. Chem. Soc.*, 1995, **117**, 2651.
- 14 F. Miyaji, S. A. Davis, J. P. H. Charmant and S. Mann, *Chem. Mater.*, 1999, **11**, 3021.
- 15 F. Tang, X. Huang, L. Wang and J. Kuo, *Nanostruct. Mater.*, 1999, **11**, 861.
- 16 H. Yang, G. Vovk, N. Coombs, I. Sokolov and G. A. Ozin, *J. Mater. Chem.*, 1998, **8**, 743.
- 17 C. Sanchez, J. Livage, M. Henry and F. Babonneau, *J. Non-Cryst. Solids*, 1988, **100**, 65.
- 18 H. Izutsu, F. Mizukami, P. K. Nair, Y. Kiyozumi and K. Maeda, *J. Mater. Chem.*, 1997, **7**, 767.